Molecular Phylogenetics and Evolution
Vol. 18, No. 3, March, pp. 386–403, 2001
doi:10.1006/mpev.2000.0883, available online at http://www.idealibrary.com on IDEAL®

A Combined Molecular Approach to Phylogeny of the Jumping Spider Subfamily Dendryphantinae (Araneae: Salticidae)

Marshal C. Hedin[1] and Wayne P. Maddison

Department of Ecology & Evolutionary Biology, University of Arizona, Tucson, Arizona 85721

Received March 17, 2000; revised October 1, 2000; published online January 23, 2001

Four gene regions were sequenced for 30 species of jumping spiders, most from the subfamily Dendryphantinae, to investigate their molecular phylogeny and evolution. These are three regions from the mitochondria (ca. 560 bp of 16S plus adjacent tRNA, 1047 bp of cytochrome oxidase 1 (CO1), and 414 bp of NADH1 (ND1) and one region from the nuclear genome (ca. 750 bp of 28S). Parsimony and likelihood analyses of these gene regions separately and together support the monophyly of the dendryphantines as delimited previously by morphological characters. A group of elongate-bodied genera are placed as basal among the dendryphantines, and previously proposed relationships of *Poultonella*, *Paraphidippus*, and *Sassacus vitis* are confirmed. Comparison of overall rates of molecular evolution indicates striking differences across the gene regions, with highest divergence in ND1, CO1, 16S, and 28S in decreasing order. All four regions are characterized by both within- and among-site rate variation. Phylogenetic results from CO1 conflict conspicuously with phylogenetic results from the other genes and morphological data. Attempts to account for potential sources of this conflict (e.g., accommodating biased base composition, high homoplasy, within- and among-site rate variation, etc.) are largely unsuccessful.

Key Words: **molecular phylogeny; Salticidae; cytochrome oxidase; incongruence; homoplasy; sequence alignment; secondary structure; ribosomal DNA.**

INTRODUCTION

The jumping spiders (Salticidae) are a diverse group, including not only more described taxa than any other spider family (estimates of ca. 4400 species in 490 genera; Coddington and Levi, 1991) but also extraordinary diversity in morphology, behavior, and predatory ecology (e.g., Jackson, 1982, 1986; Jackson and Pollard, 1996). There has been limited success in understanding the phylogenetic relationships of these spiders, perhaps because of this overwhelming diversity. The classifications of both Simon (1901) and Proszynski (1976) are based largely on single-character systems (dentition on the lower margin of the chelicerae and characteristics of genitalia, respectively) and, although both works clearly represent key progress, we might expect considerable remaining phylogenetic uncertainty, given such a large number of taxa.

More recently, the consideration of additional character systems has clarified some aspects of salticid phylogeny. Several workers (e.g., Blest and Sigmund, 1984; Wanless, 1984; Maddison, 1988, 1996) have discovered congruent character support for a basal subdivision in the family, separating the "primitive" lyssomanines and spartaeines from the bulk of the taxonomic diversity in the family (the salticines). Maddison (1987, 1988, 1996) discussed relationships within the salticines, proposing delimitations of the subfamilies Heliophaninae, Plexippinae, and Dendryphantinae, but limits of many other subfamilies remained obscure. Relationships among salticine subfamilies are similarly unclear, with the condition of the embolus–tegulum articulation ("fixed" versus "free") perhaps representing a major phylogenetic subdivision (Maddison, 1988, 1996). The one aspect of salticid phylogeny that is crystal clear is that more research effort is needed.

We have recently begun to collect molecular data to address phylogenetic problems in the Salticidae. Here we present results for one such problem, focusing on the phylogenetic relationships of a representative sample of genera of subfamily Dendryphantinae. The dendryphantines, a predominantly New World group, comprise several hundred species, spread across ca. 60 genera (see Table 1 of Maddison, 1996). Most dendryphantines have a "standard" salticid body form, although many taxa are specialized as ant, bird-dropping, or beetle mimics. The dendryphantines are one of very few salticid groups having received recent phylogenetic attention (Maddison, 1988, 1996). Dendryphantines are salticines and share a counterclockwise-

[1] To whom correspondence should be addressed at Department of Biology, San Diego State University, San Diego, CA 92182-4614. Fax: (619) 594-5676. E-mail: mhedin@sciences.sdsu.edu.

1055-7903/01 $35.00

coiled free embolus with the subfamily Euophryinae and other smaller groups. Maddison (1988, 1996) redelimited the dendryphantines and proposed three synapomorphies to support their monophyly: (i) a carina on the underside of the male chelicerae, (ii) male palpus with a compacted and hidden embolus coil, and (iii) S-shaped epigynal openings (see Figs. 10, 3, and 5, respectively, of Maddison, 1996). None of these proposed synapomorphies is without homoplasy, for there are genera tentatively placed in the subfamily that lack one or more of these features. In addition to this subfamilial delimitation, Maddison hinted at generic interrelationships within the subfamily. Although providing no formal phylogenetic analysis, a character matrix available for phylogenetic interpretation is presented (Table 2 of Maddison, 1996), along with comments on potential character support for various generic groupings.

These morphology-based phylogenetic hypotheses provide our molecular studies with a basis for informed taxonomic sampling of the subfamily and relatives. Based on this information we have gathered DNA sequence data for 27 salticid genera, two-thirds of which were considered dendryphantines by Maddison (1996). We also use the prior hypotheses as a point of comparison, considering agreement (or lack thereof) in phylogenetic relationships both deep (e.g., monophyly of the subfamily) and shallow (e.g., *Poultonella* plus *Tutelina;* Maddison, 1996) to help assess the phylogenetic "behavior" of molecular data from four different gene regions. This assessment is important, as our dendryphantine work represents one of the first studies to consider the comparative utility of different molecular markers in resolving spider phylogeny. Because this comparative utility is highly contingent upon molecular evolutionary dynamics, this paper emphasizes basic structural features of these gene regions and highlights differences in rates and patterns of molecular evolution. These considerations will hopefully allow spider systematists to make more informed decisions regarding molecular phylogenetic sampling in future studies.

METHODS AND MATERIALS

The taxon sample includes a total of 32 species representing 27 genera (Table 1). Our sampling of particular species within a genus was based primarily on convenience, rather than on any perceived special placement of the species within the genus. The generic sample includes 20 taxa that are listed as dendryphantines by Maddison (1996), constituting approximately one-third of the generic diversity in the subfamily. All of these taxa are distributed in the New World, reflecting the biogeographical bias observed in the subfamily (only three small generic groups are Old World). The dendryphantine sample includes many taxa of special interest. For example, *Mabellina* (listed as a dendryphantine by Maddison (1996)) lacks all of the proposed synapomorphies for the subfamily but has a general body form and markings like those of other dendryphantines. The sample also includes several genera considered as dendryphantines by Maddison (1996) but placed elsewhere by other authors. These include *Beata, Bellota, Tutelina,* and *Zygoballus,* placed in Simon's (1901, 1903) Simaetheae, Synageleae, Chysilleae, and Zygoballeae, respectively.

Ten genera were sampled that fall outside of Maddison's concept of the Dendryphantinae (Table 1). The genera *Itata, Attidops, Admestina,* and *Peckhamia* are similar in sharing a counterclockwise-coiled, free embolus, and Maddison (1988, 1996) suggests the possibility that *Attidops, Admestina,* and *Peckhamia* may, in fact, represent derived dendryphantines. Our outgroup sampling is also in part based on our unpublished molecular phylogenetic work in other parts of the family. This research suggests that members of the subfamily Marpissinae (with a fixed embolus) are close relatives of dendryphantines, but that other taxa sharing a counterclockwise-coiled, free embolus (e.g., *Phlegra, Sandalodes,* euophryines) are in fact distant. Correspondingly, we have included a sample of marpissines, including *Platycryptus, Marpissa,* and an undescribed neotropical marpissine genus, but have excluded others. This unpublished work also suggests that the taxa *Thiodina, Heratemita,* and *Neon* are distant relatives of dendryphantines; we have designated *Thiodina* as the outgroup taxon in all phylogenetic analyses.

Entire legs were taken from spiders and preserved in either 100% EtOH or TE buffer and stored at −80°C. For a minority of specimens, tissues in addition to legs were used (e.g., abdomen, cephalothorax). Otherwise-intact spiders are preserved as voucher specimens (in 100% ETOH at −80°C) in the personal collection of W.P.M. Genomic DNAs were extracted from tissues using a CTAB extraction protocol (Shahjahan *et al.,* 1995). Diluted genomics were used in PCRs to generate DNA fragments from four gene regions, including partial sequences for the mitochondrially encoded cytochrome oxidase I (CO1), NADH dehydrogenase subunit I (ND1), and 16S genes and the nuclear-encoded large subunit (28S) ribosomal repeat. The ~1-kb region spanning the 3′ end of 16S to the middle of ND1, with an intervening $tRNA^{LEU\ (CUN)}$, was amplified either as a single fragment using the primers N1-J-12261 (Hedin, 1997a) with LR-N-13398 (Simon *et al.,* 1994) or as two overlapping fragments using 12261 with LR-N-12945 (Hedin, 1997b) and 13398 with N1-J-12581 (5′-CCT TTA ACG AAT TTG AAT ATA-3′; this study). Most CO1 PCR fragments were amplified using the primer combination C1-J-1718 (Simon *et al.,* 1994) with C1-N-2776 5′-GGA TAA TCA GAA TAT CGT CGA GG-3′. Some products were amplified as two smaller pieces

TABLE 1

Taxon Sample

Taxon	Locality	ND1 Access. No. (Seq Len)	16S Access. No. (Seq Len)	CO1 Access. No. (Seq Len)	28S Access. No. (Seq Len)
Thiodina sp.	Arizona: Tucson	(414) AF328017	(556) AF327958	(1032) AF327987	(740) AF327930
Neon nelli G. & E. Peckham	Massachusetts: Jamaica Plain	(414) AF328018	(554) AF327959	(1047) AF327988	(743) AF327931
Itata sp.	Ecuador: Machalilla NP	(414) AF328019	(557) AF327960	(1047) AF327989	(752) AF327932
Attidops youngi G. & E. Peckham	Missouri: Valley View Glade	(414) AF328020	(558) AF327961	(1047) AF327990	(757) AF327933
*Heratemita alboplagiata** Simon	Philippines	(414) AF328021	(551) AF327962	(1047) AF327991	(749) AF327934
Platycryptus undatus DeGeer	Florida: Newnan's Lake	(414) AF328022	(553) AF327963	(1047) AF327992	(743) AF327935
Marpissa pikei G. & E. Peckham	Arizona: W of Nogales	(408) AF328023	(553) AF327964	(1047) AF327993	(748) AF327936
Unident. marpissine	Costa Rica: La Selva	(414) AF328024	(562) AF327965	(1047) AF327994	(763) AF327937
Peckhamia sp.	Arizona: Atascosa Peak	(414) AF328025	(556) AF327966	(1047) AF327995	(746) AF327938
Admestina sp.	South Carolina: Clemson	NA	NA	(1047) AF327996	NA
Pelegrina chalceola Maddison	Arizona: Santa Rita Mts.	(414) AF328026	(553) AF327967	(969) AF327997	—
Pelegrina verecunda Chamberlin & Gertsch	Arizona: Chiricahua Mts.	—	—	—	(745) AF327939
Phidippus sp.	Arizona: Santa Rita Mts.	(414) AF328027	(553) AF327968	(1047) AF327998	—
Phidippus sp.	Utah: LD Ranch	—	—	—	(745) AF327940
*Beata magna** G. & E. Peckham	Peru: Yanamono	(414) AF328028	(553) AF327969	(975) AF327999	(745) AF327941
Eris militaris Keyserling	Ontario: Kirkland	(414) AF328029	(554) AF327970	(966) AF328000	(743) AF327942
Terralonus mylothrus Chamberlin	Colorado: Avery Peak	(414) AF328030	(554) AF327971	(1047) AF328001	(745) AF327943
Zygoballus rufipes G. & E. Peckham	Massachusetts	(414) AF328031	(552) AF327972	(1047) AF328002	(744) AF327944
*Rudra wagae** Taczanowski	Ecuador: Cuyabeno	(414) AF328032	(195) AF327973	(1047) AF328003	(746) AF327945
Phanias sp.	Arizona: Mt. Hopkins	(414) AF328033	(555) AF327974	(1047) AF328004	(744) AF327946
Hentzia palmarum Hentz	Texas: Independence Creek	(414) AF328034	(552) AF327975	(1047) AF328005	NA
Bellota cf. *wheeleri* G. & E. Peckham	Chiapas: Pto. Arista	(414) AF328035	(553) AF327976	(1047) AF328006	(744) AF327947
Mabellina prescotti Chickering	Jalisco: Chamela	(414) AF328036	(554) AF327977	(1020) AF328007	(749) AF327948
Paradamoetas sp.	Chiapas: Pto. Arista	(414) AF328037	(195) AF327978	(1047) AF328008	(747) AF327949
Poultonella alboimmaculata G. & E. Peckham	Texas: Falcon Lake	(414) AF328038	(554) AF327979	(1047) AF328009	(744) AF327950
Sassacus sp.*	Ecuador: Cuyabeno	(414) AF328039	(203) AF327980	(1047) AF328010	(744) AF327951
Rhetenor cf. *texanus* Gertsch	Chiapas: Pto. Arista	(414) AF328040	(553) AF327981	(1047) AF328011	(746) AF327952
Sassacus papenhoei G. & E. Peckham	Arizona: Yuma County	(414) AF328041	(554) AF327982	(1047) AF328012	(747) AF327953
Tutelina hartii Emerton	Oklahoma: Wah-Sha-She SP	(414) AF328042	(193) AF327983	(1047) AF328013	(744) AF327954
Sassacus vitis Cockerell	California: Beaver Creek	(414) AF328043	(552) AF327984	(1047) AF328014	(747) AF327955
Paraphidippus aurantius Lucas	Arizona: Santa Rita Mts.	(414) AF328044	(556) AF327985	(1047) AF328015	(745) AF327956
Messua limbata Banks	Arizona: Pinaleno Mts.	(414) AF328045	(554) AF327986	(1047) AF328016	(745) AF327957

Note. Taxon sample used in molecular phylogenetic analysis. Some species identifications, marked with an asterisk, are tentative. For both *Pelegrina* and *Phidippus*, different species were used to amplify different gene regions. These data were merged as a single taxon for phylogenetic analysis.

using the primer combinations of C1-J-1751 "SPID" 5′-GAG CTC CTG ATA TAG CTT TTC C-3′ with C1-N-2568 5′-GCT ACA ACA TAA TAA GTA TCA TG-3′ and C1-J-2309 5′-TTT ATG CTA TAG TTG GAA TTG G-3′ with C1-N-2776 (all this study). The approximately 800-bp fragment of 28S, spanning divergent domains D2 and D3, was amplified using the primers 28S "O" 5′-GAA ACT GCT CAA AGG TAA ACG G-3′ and 28S "C" 5′-GGT TCG ATT AGT CTT TCG CC-3′ (this study). PCR experiments included an initial 95°C denaturation followed by 35 cycles of 30 s at 95°C, 30 s at either 48°C (16S/ND1), 52°C (CO1), or 55°C (28S), 45 s at 72°C + 3 s per cycle, with a final 10-min extension at 72°C. All PCRs included *Taq*Start Antibody (Clontech Laboratories), using dilutions suggested by the manufacturer; amplification of the GC-rich 28S region was further enhanced with the MasterAmp PCR optimization kit (Epicentre Technologies). Polyacrylamide gel-purified PCR products (Sambrook *et al.*, 1989) were directly sequenced using automated techniques on ABI 373 and 377 machines. Both strands were determined for all 28S sequences. Mitochondrial fragments were sequenced primarily in a single direction, but the use of various primer combinations (see references above) allowed for up to 60% sequence overlap.

DNA sequences were imported as text files into a sequence editor (either SeqApp V1.9a (Gilbert, 1992) or a beta version of MacClade 4 (Maddison and Maddison, 1999)) checked by eye against hard-copy chromatograms, and rechecked against complementary-strand sequence (if available). Edited sequences for each data partition were compiled into a single data file for multiple alignment. Protein-coding data, containing no in-

ternal length variation, were aligned manually. Both ribosomal fragments (16S and 28S) included length variation over the taxa sampled and were aligned automatically using the program ClustalX (Higgins and Sharp, 1988). All initial pairwise alignments were conducted using the "fast, approximate" option. Multiple alignments were carried out using default transition "weights" of 0.5, while varying the gap opening/gap extension costs over a range that included ratios of 8/2, 20/2, 8/4, 24/6, and 24/4. These ratio values, ranging from 2 to 10, were found to span a parameter space including both relatively "gappy" (e.g., 8/2) and "compressed" (e.g., 24/6) alignments.

Phylogenetic analyses were conducted using various beta versions of PAUP* V4.0 (b2a–b4a; Swofford, 1999) in combination with beta MacClade 4 (Maddison and Maddison, 1999). Parsimony analyses were carried out on representative matrices (see below) for each of the length-variable data partitions, the separate CO1 and ND1 character partitions, and matrices comprising concatenations of all data partitions. Parsimony searches were heuristic, with tree bisection–reconnection (TBR) branch-swapping and multiple random addition sequence replicates. Relative support of reconstructed clades was evaluated via the nonparametric bootstrap (Felsenstein, 1985), based on analyses comprising 1000 replicates of a heuristic search (as above, but with fewer random addition sequence replicates). Global (i.e., tree-wide) phylogenetic congruence across data partitions was assessed in the context of parsimony using the PAUP* implementation of the incongruence length difference (ILD) test (Farris *et al.*, 1995). Following Cunningham (1997a), invariant characters were excluded prior to ILD data randomizations.

Maximum-likelihood phylogeny estimates included an initial evaluation of alternative models of DNA sequence evolution, with models differing in parameters associated with base composition (equal versus not) and number of substitutional classes (one-, two-, or six-parameter). Likelihood values of nested models, estimated over a common (most-parsimonious) tree topology using the TREESCORES feature of PAUP* (Swofford, 1999), were compared using the MODELTEST (Posada and Crandall, 1998) implementation of the likelihood ratio test. Incorporation of among-site rate variation, following either the invariable-sites method (%I) alone or a combination with the discrete gamma distribution (Γ), was considered prior to increasing the number of substitutional classes from two to six (see Cunningham *et al.*, 1998). Using a best-fit model, estimates of both maximum-likelihood model parameters and trees were conducted using a successive approximations approach, following suggestions of Swofford *et al.* (1996). This approach included an estimation of model parameters on an initial tree derived from a weak search (i.e., a partial heuristic search, no random addition sequence replicates). These parameter estimates were then fixed while searching for better trees using a more thorough TBR heuristic search incorporating five multiple random addition sequence replicates. If trees of higher likelihood were found, parameter estimates were reoptimized and fixed anew, followed by another thorough search. Searches were deemed complete when trees of approximately equal likelihood were found in successive iterations.

RESULTS

Sequence data from four gene regions, totaling about 2.7 kb per taxon, were gathered for each of the 30 taxa included in phylogenetic analyses (Table 1). Exceptions include *Admestina* (CO1 only) and *Hentzia* (no 28S). For both *Pelegrina* and *Phidippus*, different species were used to amplify different gene regions; these data were merged as a single taxon for phylogenetic analysis. Some ND1, CO1, and 16S plus tRNA sequences are incomplete at either the 5′ or the 3′ ends for a small number of taxa (Table 1); these taxa were included with missing data in phylogenetic analyses. All sequences have been deposited in GenBank (Table 1).

As expected, mitochondrial sequences are relatively AT rich, whereas 28S sequences are GC rich (Table 2). For each data partition, PAUP* χ^2 analyses (uncorrected for phylogeny; see Swofford, 1999) were conducted to test for variation in base composition across taxa, considering either all sites or variable sites only (Table 2). These tests suggest that observed base compositions are homogeneous across taxa, with the exception of CO1 variable positions that appear to deviate from the stationarity assumption (Table 2). Position-specific analyses of all sites suggest that this nonstationarity is concentrated at third positions, where percentage A + T values range from 0.814 to 0.963. The taxon sample is homogeneous in CO1 base composition at both first and second positions, with average percentage A + T values (0.582 and 0.603, respectively) that also indicate less base compositional bias.

16S + tRNA Alignment and Characteristics

Five different gap opening/extension costs result in four distinct 16S + tRNA alignments (20/2 = 8/2), with aligned lengths ranging from 573 to 576 bp. Because we had no *a priori* basis for choosing one alignment over another, we could have either used all of the alignments or used some external criterion in choosing one or some subset of the alignments. We used phylogenetic congruence as an "external" criterion by comparing phylogenetic results from each alignment matrix alone to results based on a concatenation of all such matrices (i.e., an elision matrix; Wheeler *et al.*, 1995), treating gaps as a fifth base in all tree searches. In principle, an elision matrix should generally recover relationships that are robust to alignment differences, but it is also unwieldy. Hence, we utilized that align-

TABLE 2

Base Composition Information

	CO1	ND1	16S + tRNA	28S
A	0.218/**0.250**/0.274	0.343/**0.362**/0.389	0.379/**0.400**/0.428	0.159/**0.171**/0.178
	0.271/***0.348***/*0.405*	*0.349*/***0.382***/*0.429*	*0.369*/***0.428***/*0.490*	*0.131*/***0.171***/*0.193*
C	0.115/**0.122**/0.130	0.100/**0.140**/0.176	0.109/**0.122**/0.138	0.289/**0.296**/0.310
	0.035/***0.051***/*0.068*	*0.075*/***0.147***/*0.210*	*0.072*/***0.099***/*0.125*	*0.273*/***0.310***/*0.354*
G	0.173/**0.189**/0.211	0.092/**0.099**/0.106	0.119/**0.129**/0.158	0.346/**0.354**/0.369
	0.096/***0.143***/*0.196*	*0.038*/***0.050***/*0.080*	*0.042*/***0.060***/*0.095*	*0.240*/***0.268***/*0.310*
T	0.422/**0.438**/0.448	0.357/**0.400**/0.444	0.328/**0.349**/0.371	0.160/**0.178**/0.187
	0.424/***0.458***/*0.484*	*0.349*/***0.421***/*0.500*	*0.369*/***0.411***/*0.456*	*0.179*/***0.251***/*0.290*
***P* values**	0.99	0.99	1.00	1.00
	0.015	*0.32*	*0.99*	*0.99*

Note. Included are low values/means (boldface)/high values of observed base frequencies among the sampled taxa for each data partition, considering either all sites (above, plain text) or variable sites only (below, italicized). *P* values resulting from χ^2 tests of homogeneity (PAUP* implementation, Swofford, 1999) are uncorrected for phylogeny.

ment matrix most similar to the elision matrix for more derived analyses. This similarity was assessed in two ways, first by comparing the number of nodes in common between consensus parsimony trees from independent versus elision matrices (Fig. 1). The "24/4" alignment result is most similar to the elision result, sharing 20 of 25 nodes in common. Other alignments share between 7 and 13 nodes in common. Similarity was also assessed by calculating symmetric-difference distances (Swofford, 1999) between sets of most-parsimonious trees resulting from independent versus elision analyses. Such average distances are less for the 24/4 alignment than for any other alignment (4.67 versus 12.53–34.1), again suggesting that this matrix might be justifiably used as a surrogate for the elision matrix. The 24/4 alignment is relatively "compressed," with only 38 of 573 total sites including indel character states (i.e., gaps).

The distribution of variable positions (including positions involving indels) across the 16S plus tRNA region was assessed in light of a proposed secondary structure (Fig. 2), following a model proposed for the salticid genus *Habronattus* (Masta, 2000a). Our secondary structure hypothesis is very similar to that proposed for *Habronattus* and is supported by the observation of 25 proposed stem positions that show evidence for compensatory mutation (Fig. 2). Overall, both 16S and tRNA molecules show evidence for among-site rate variation, with regions of both high variability (e.g., upstream of the peptidyl transferase center) and extreme conservation (e.g., 3′ stems of the peptidyl transferase center). A mapping of the positions involving indels suggests that such sites fall within proposed loop or unpaired regions (Fig. 2), with a concentration of indels in the spacer region separating 16S from tRNA and at the 3′ end of the tRNA molecule (amino-acyl arm). The observation of truncated tRNAs with unstable amino-acyl stems in dendryphantines is consistent with findings for *Habronattus* (Masta, 2000a), and may prove to be widespread in spiders.

28S Alignment and Characteristics

The alignment parameter space explored results in four distinct 28S alignments (24/4 = 24/6), with lengths ranging from 771 to 791 bp. Following the same logic as presented above, the "20/2" alignment is judged as most similar to the elision matrix, based both on number of nodes in common (nine versus six to eight; Fig. 3) and on lower average symmetric-difference distances (21.12 versus 24.49–27.33). This alignment is relatively compressed, with only 52 of 773 aligned positions including gaps. As above, patterns of variation in the 28S data can be assessed in light of a secondary structure model. The hypothesis proposed for dendryphantines (Fig. 4) is based on comparison to the universal model of Schnare *et al.* (1996). This model is supported by the observation of apparent compensatory mutations at 29 hypothesized stem positions (Fig. 4). Levels of sequence variability differ across the region sequenced, the majority of variable positions mapping to either the D2 or the D3 "divergent domains," with little variation in the "core" domain. Positions requiring indels are concentrated within proposed loop or unpaired regions of the D2 and D3 regions (Fig. 4).

CO1 Data Characteristics

CO1 nucleotide and amino acid data can be fitted to a two-dimensional structural model (Fig. 5) analogous to that proposed for hexapods (Lunt *et al.*, 1996). Considering levels of nucleotide variation in light of this model reveals differences across structural domains, particularly at 1st and 3rd codon positions (Fig. 5, bottom). For example, although variation at 3rd positions is uniformly high, the average number of parsimony-reconstructed changes per position ranges from 3.8 to 6.8 (calculated separately for each domain). The

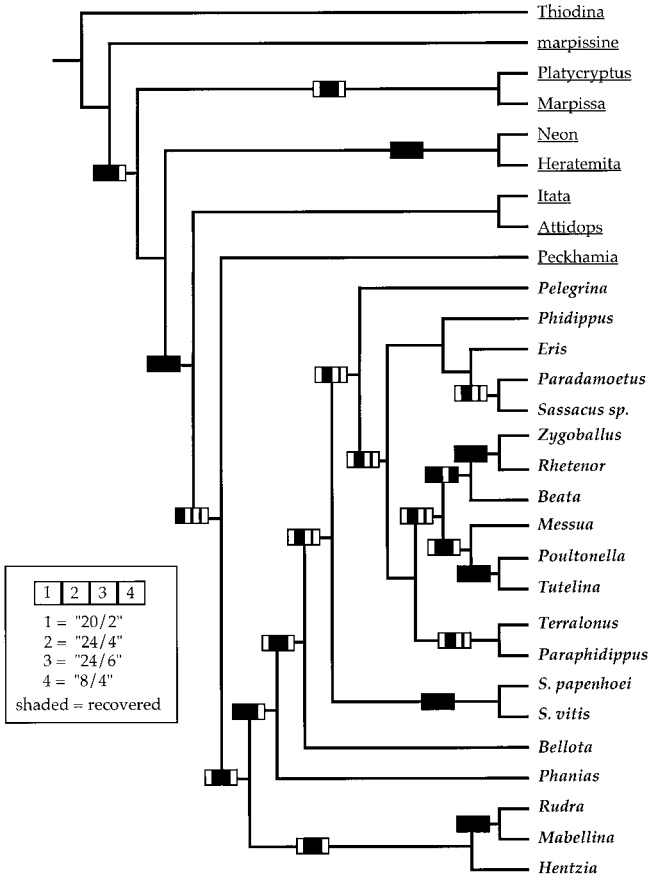

FIG. 1. Single most-parsimonious tree (L = 4315) resulting from a concatenated matrix of four distinct 16S + tRNA alignments (elision matrix). Parsimony results based on heuristic search with TBR branch-swapping, 100 random addition search replicates, all gaps treated as a "fifth state." Mapped onto the elision tree are results of independent heuristic searches (as above) for each of the four distinct alignments. For each node in the elision tree we indicate whether or not the same node was recovered in the strict consensus tree of independent alignment analyses—five elision nodes (unlabeled) are not found in any such trees. The 24/4 alignment results in trees with the greatest number of nodes in common (20 of 25—because we designated *Thiodina* as outgroup, we do not count the basal node in the tree). Taxa in boldface italicized font are considered to be dendryphantines, sensu Maddison (1996).

correspondence between the structural domain and the patterns of nucleotide variability is generally similar to that reported for hexapods (Lunt *et al.*, 1996). More variable regions are spread across transmembrane helices (e.g., M5 and M9), external loops (e.g., E2), and internal loops (e.g., I2 and I5), whereas conserved regions typically correspond to transmembrane helices (e.g., M4, M6, M8, and M10). However, patterns of variation at the amino acid level (Fig. 5, top) suggest that there are runs of either conserved or variable residues that do not correspond directly to loops or transmembrane areas (e.g., the longest runs of conserved residues include E2 plus M4 and M5 plus E3).

ND1 Data Characteristics

Although protein structural data are unavailable for the ND1 region, patterns of nucleotide variation are nonetheless informative (Fig. 6). As expected, 3rd positions are most variable, with an average number of parsimony-reconstructed steps per site of 2.17, 0.89, and 6.02 for 1st through 3rd positions, respectively. This average level of variability is similar to that observed for more variable CO1 domains (see above). Figure 6 also clearly indicates regional differences in nucleotide variability across ND1, with a relatively conserved region between positions 30 and ca. 180. This region is also characterized by reduced amino acid variability.

Individual Partition Phylogenetic Analyses

We present results from two types of phylogenetic analyses that might be viewed as widely separate points along an extensive analytical continuum. These include parsimony analyses with characters treated as unordered and of equal weight, including gaps as a fifth state (if applicable). This set of analyses makes fewer explicit assumptions than the likelihood analyses also presented. Likelihood analyses were conducted for each partition using "best-fit" models for the data. For all partitions, a parameter-rich GTR model was deemed to have a significantly higher likelihood as assessed using the likelihood ratio test (results not shown). Incorporation of among-site rate variation (GTR + I + Γ) further improved the likelihood of all models. These analyses differ most from parsimony in incorporating both within- and among-site rate variation and in the treatment of indels (ignored in ML analyses). Neither set of analyses included special treatment of nonindependent sites apparently involved in compensatory mutation (see above).

Results of separate parsimony analyses are summarized in Fig. 7, showing a strict consensus tree for each of the four data partitions. In general, bootstrap proportion (BP) values based on individual partitions are low (most BP values $<$50%), with higher values restricted to sister relationships toward the tips of trees. There are no cases in which strongly supported clades (e.g., BP $>$70%) are in conflict across data partitions. At least three of the partitions are consistent in recovering dendryphantines as monophyletic. The exception is the relatively homoplasious CO1 data, with trees characterized by apparently basal dendryphantines (*Rudra, Mabellina, Rhetenor, Zygoballus, Phanias, Hentzia;* see Figs. 10 and 11) intermixed with proposed outgroup taxa, in addition to a (*Peckhamia, Paradamoetus*) sister relationship. CO1 parsimony trees with proposed dendryphantines constrained to form an exclusive monophyletic clade require an increase in length of 14 steps (less than 0.010% of the total tree length).

Results of the successive-approximations maximum-

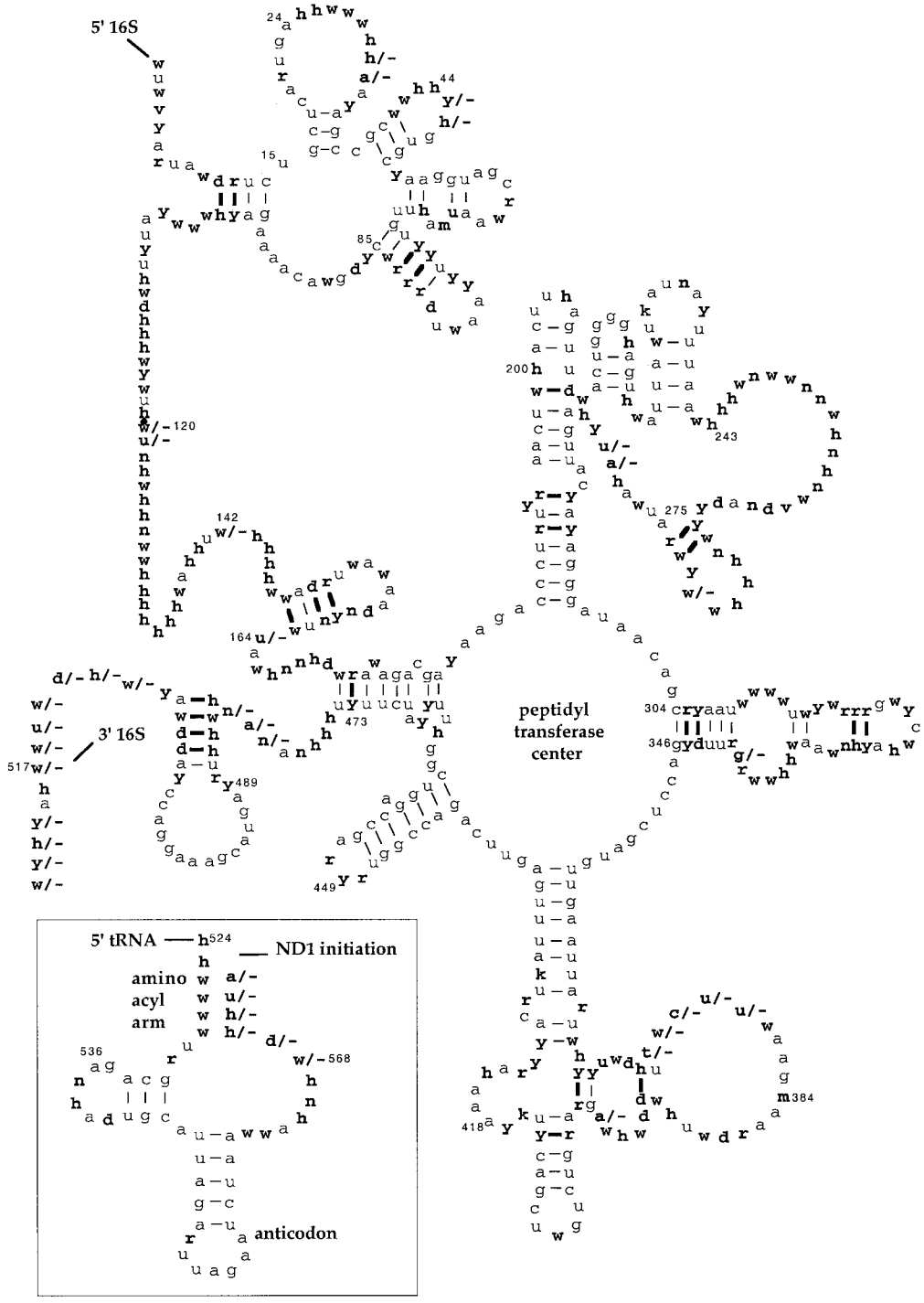

FIG. 2. Proposed secondary structure for 16S and tRNA leucine (CUN), following model of Masta (2000a). Variable sites are indicated by boldface IUPAC symbols. Dashes represent Watson–Crick pairings or G-T bonds; larger dashes indicate apparent compensatory mutations. As proposed by Masta (2000a), the tRNA structure in these spiders is characterized by an apparently unstable amino-acyl arm and missing TΨC and variable arms. A 4-bp overlap is proposed to exist between the 3′ end of tRNA leucine (CUN) and the initiation codon of ND1.

likelihood searches are presented as Figs. 8 and 9. Most searches stabilized after two iterations following an initial weak tree search, with ending log likelihood tree scores within 10 of initial tree scores. Similar to parsimony analyses, CO1 is the only partition that fails to recover a monophyletic dendryphantine clade, although the sole "violation" is the placement of a long-branched *Peckhamia* well within a dendryphantine

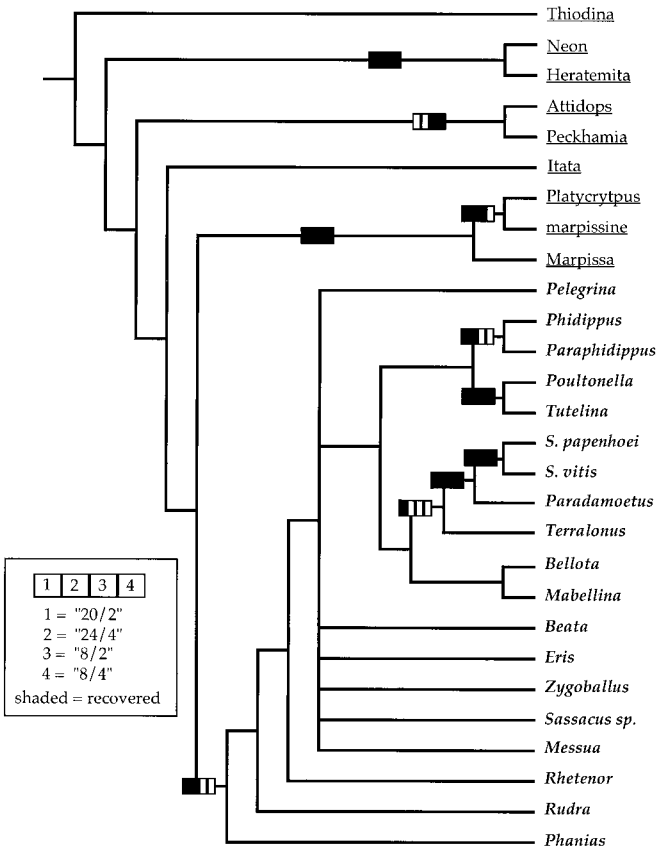

FIG. 3. Strict consensus of most-parsimonious trees (N = 2, L = 2803) resulting from a concatenated matrix of four distinct 28S alignments. Parsimony results based on heuristic search with TBR branch-swapping, 100 random addition search replicates, all gaps treated as a fifth state. Mapped onto the elision consensus tree are results of independent heuristic searches (as above) for each of the four alignments. For each node in the elision tree we indicate whether or not the same node was recovered in the consensus of independent alignment analyses—10 elision nodes (unlabeled) are not found in any such trees. The 20/2 alignment results in trees with the greatest number of nodes in common (9 of 20, ignoring the node separating *Thiodina* from the other taxa).

clade (Fig. 9). The (*Peckhamia, Paradamoetus*) sister relationship recovered in CO1 parsimony and likelihood analyses is never recovered in analyses of other individual data partitions and does not recur in combined analyses with CO1 included (Figs. 10 and 11).

Combined Phylogenetic Analyses

Consistent with the individual parsimony analyses presented above, results of standard parsimony ILD analyses (all characters included and treated as unordered) suggest that three of four data partitions are mutually congruent (all P values > 0.01) but that the CO1 partition is incongruent with all others (all P values < 0.001; Table 3). Focusing specifically on the apparent outlier CO1 data, we investigated the potential source of this conflict in phylogenetic signal via alternative ILD analyses. These exploratory analyses were conducted primarily to provide further insight into characteristics of the CO1 data partition, rather than as strict tests of data combinability.

Given the suspicious placement of *Peckhamia* in both CO1 parsimony and likelihood trees, we ran ILD analyses with this taxon removed. This is a crude way of assessing whether the placement of one taxon is disproportionately responsible for measures of global incongruence (Poe, 1996; Thornton and DeSalle, 2000). ILD analyses excluding *Peckhamia* had little influence on significance values, with all P values < 0.005 (ILD search parameters: 1000 data randomizations, each with TBR heuristic, three random addition sequence replicates, no invariant, gaps as "fifth"). These results, however, do not preclude the possibility of significant localized incongruence (e.g., signal conflict involving the placement of *Peckhamia* plus relatively few other nodes), which has not been fully assessed.

We also conducted ILD analyses on CO1 matrices without 3rd positions. As indicated above, parsimony trees are characterized by apparently basal dendryphantines intermixed with proposed outgroup taxa. Perhaps saturation at 3rd positions is accounting for a majority of signal conflict at this phylogenetic depth. Results of these analyses suggest reduced incongruence between partitions (Table 3), but this "congruence" is difficult to interpret. A primary problem is that CO1 parsimony analyses without 3rd positions result in a larger number of most-parsimonious trees (157 versus 5), indicating that the resolving power of the remaining data is decreased.

Finally, following Cunningham (1997a,b), we explored a more complex "six-parameter" parsimony model, attempting to account for the obvious substitutional biases of the CO1 data (see Table 4). These analyses drastically reduce the measured incongruence of data partitions (all P values >0.85; Table 3), suggesting that some of this signal conflict is due to a mismatch between the assumptions of a standard parsimony model and the characteristics of the CO1 data. This suggestion is consistent with comparisons of trees resulting from likelihood (more complex) versus parsimony (less complex) searches (Figs. 7 and 9), with ML trees apparently more similar to trees from other data partitions. The result also suggests that, in conducting a combined analysis of all data, the incorporation of a CO1 six-parameter model might serve to neutralize or lessen phylogenetic conflict between data partitions.

Combined analyses were conducted on concatenated matrices treating all data partitions as unordered (Fig. 10) or treating all partitions as unordered except for CO1, for which six-parameter parsimony was applied (Fig. 11). Both combined analyses suggest similar dendryphantine relationships, although the mixed-model analysis lacks a (*S. vitis, S. papenhoei*) sister relationship recovered in all individual searches of all parti-

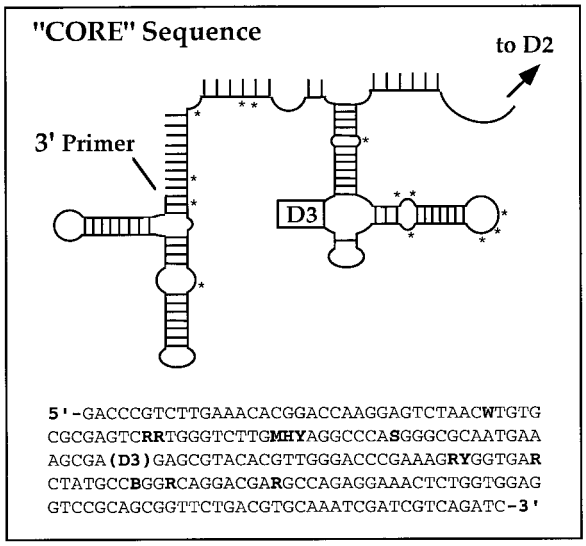

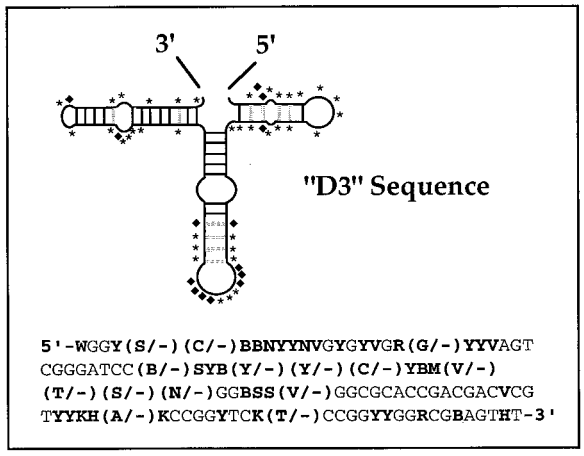

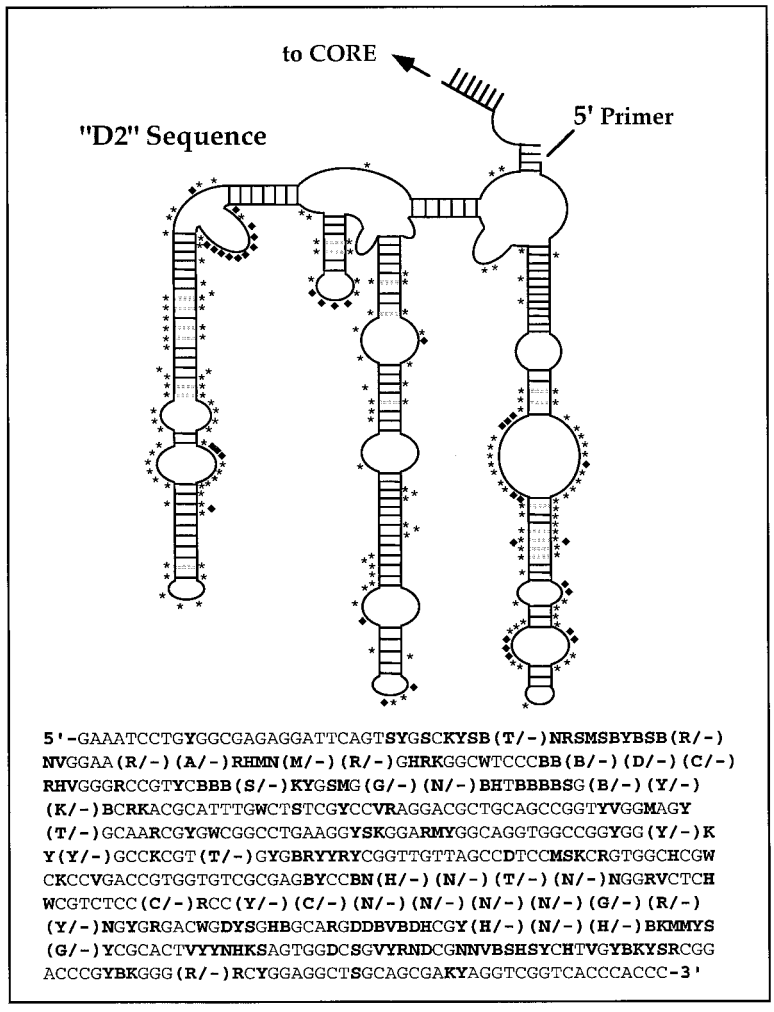

FIG. 4. Proposed secondary structural model for dendryphantine 28S data spanning divergent domains D2, D3, and an intervening "core" region. The proposed secondary structure is based on comparison to the universal models of Schnare *et al.* (1996) and is further supported by covariation of stem pairings designated by stippled bars. All stem pairings shown involve either A-T, G-C, or G-T bonds. Asterisks indicate variable sites, and diamonds indicate sites including indels.

tions except for CO1 (see Fig. 10). Furthermore, BP values from the mixed-model analysis are almost universally lower, with some nodes (e.g., the dendryphantine node) receiving no bootstrap support. The inclusion of CO1 data appears to be eroding otherwise congruent signal in this instance, even with the mixed-model assumption. Relationships outside of the dendryphantines are more resolved in the mixed-model analysis, but the resolution is not well supported and is apparently consistent only with the CO1 partition (Fig. 11). The mixed-model tree also lacks a basal (*Neon*, *Heratemita*) grouping found in other analyses (Fig. 10). In sum, it is not evident that a mixed-model analysis is lessening phylogenetic conflict between data partitions, as predicted by pairwise ILD analyses. If anything, the opposite appears true.

DISCUSSION

Patterns of Molecular Evolution

The different subsets of molecular data gathered for this project are clearly evolving under different evolutionary dynamics (i.e., they differ in rates and patterns of nucleotide substitution). Differences in overall levels of nucleotide divergence are best illustrated by consideration of pairwise divergence values for three consistently recovered sister pairings of taxa, including *S. papenhoei* + *S. vitis*, *Poultonella* + *Tutelina*, and *Zygoballus* + *Rhetenor* (see Fig. 10). All three pairings involve relatively closely related taxa, thus minimizing the potentially confounding influence of substitutional saturation in the comparisons. Consideration of these focal pairings indicates a consistent ranking of estimated pairwise values (from high to low) as follows:

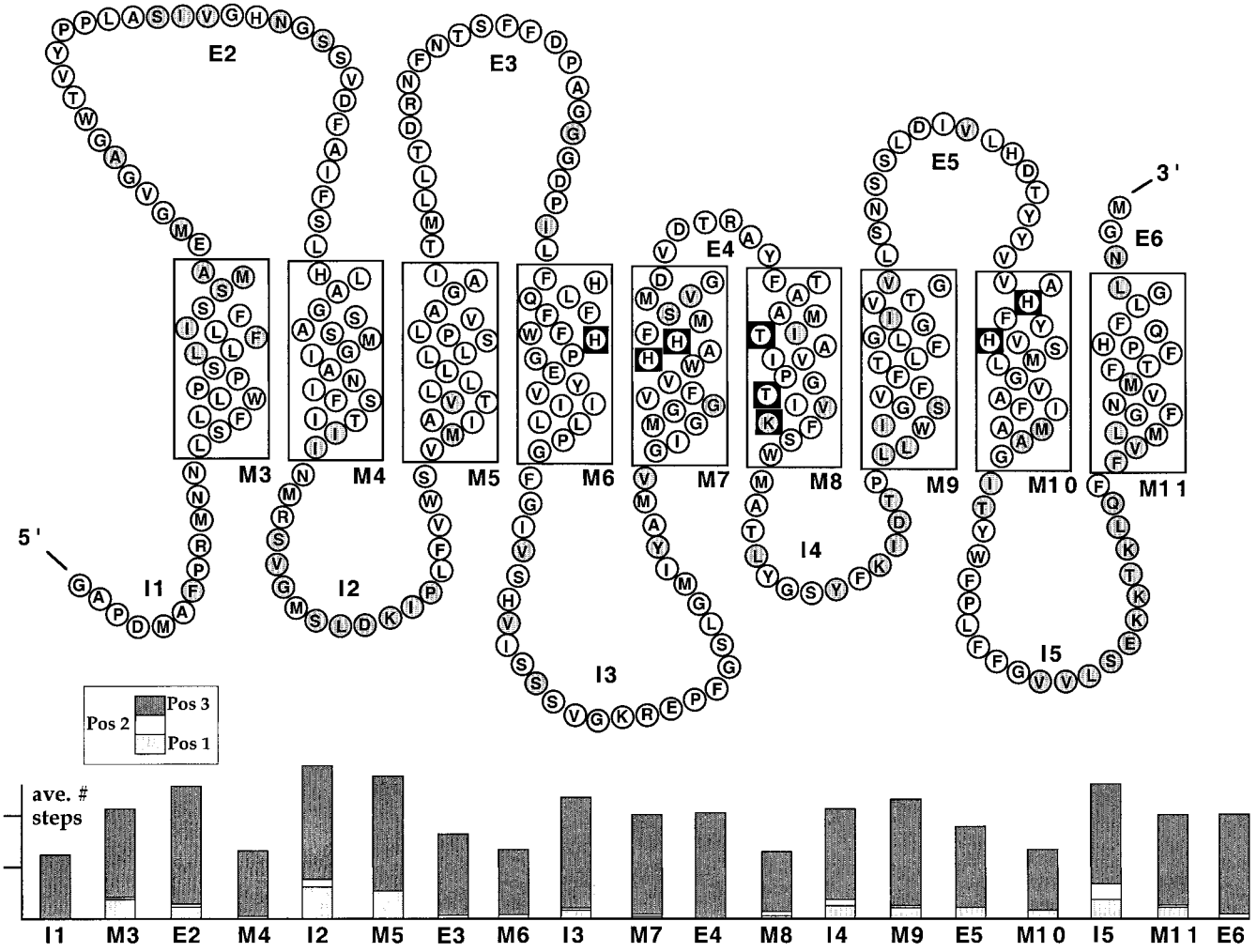

FIG. 5. (Top). Proposed structural model for dendryphantine CO1 data, following the Lunt *et al.* (1996) hypothesis for hexapods. Structural regions include both internal (I) and external (E) loops and membrane-bound helices (M). Amino acid residues shown represent a consensus of that observed, with variable residues indicated by shading. Membrane-bound residues in black boxes are proposed to have special function; amino acids at these sites are identical to conserved hexapod residues (Lunt *et al.*, 1996). Nucleotides were translated assuming the genetic code of *Drosophila* mtDNA, using a beta version of MacClade 4 (Maddison and Maddison, 1999). (Bottom) Nucleotide variation categorized by codon position and structural domain. Numbers include the average number of steps per site, estimated over the set of most-parsimonious trees for the CO1 data using MacClade.

ND1 ≫ CO1 ≫ 16S ≫ 28S. Differences in the absolute divergence values across gene regions are substantial. For example, *Poultonella* and *Tutelina* share the exact same 28S sequence but are more than 9% divergent at ND1. *Sassacus papenhoei* and *S. vitis* are less than 1% divergent at 28S but differ by almost 15% at ND1. Assuming that each sister taxa pairing shares a unique common ancestor (i.e., that the sequences have evolved over a common time frame), these differences in absolute levels of divergence necessarily reflect differences in the rates of evolution of the different sequences.

The gene regions also show differences in patterns of substitution (i.e., transition–transversion probabilities) and among-site rate variation. All four data sets show a general transition bias (Table 4), although this bias is less extreme for the 28S nuclear data. Gross differences in patterns of among-site rate variation in the protein-coding data are apparent from Figs. 5 and 6, as indicated by parsimony reconstructions of the number of steps per site categorized by codon position. As expected, essentially all 3rd sites are “free to vary”, with many fewer variable 1st and 2nd sites. Structural considerations suggest similar patterns for the ribosomal genes, with regions of conservation intermixed with regions of high variability (Figs. 2 and 4). For all four regions, ML estimates of the gamma shape parameter (using the four-category discrete approximation of Yang, 1994) indicate that some variable sites experience less change and others experience more change.

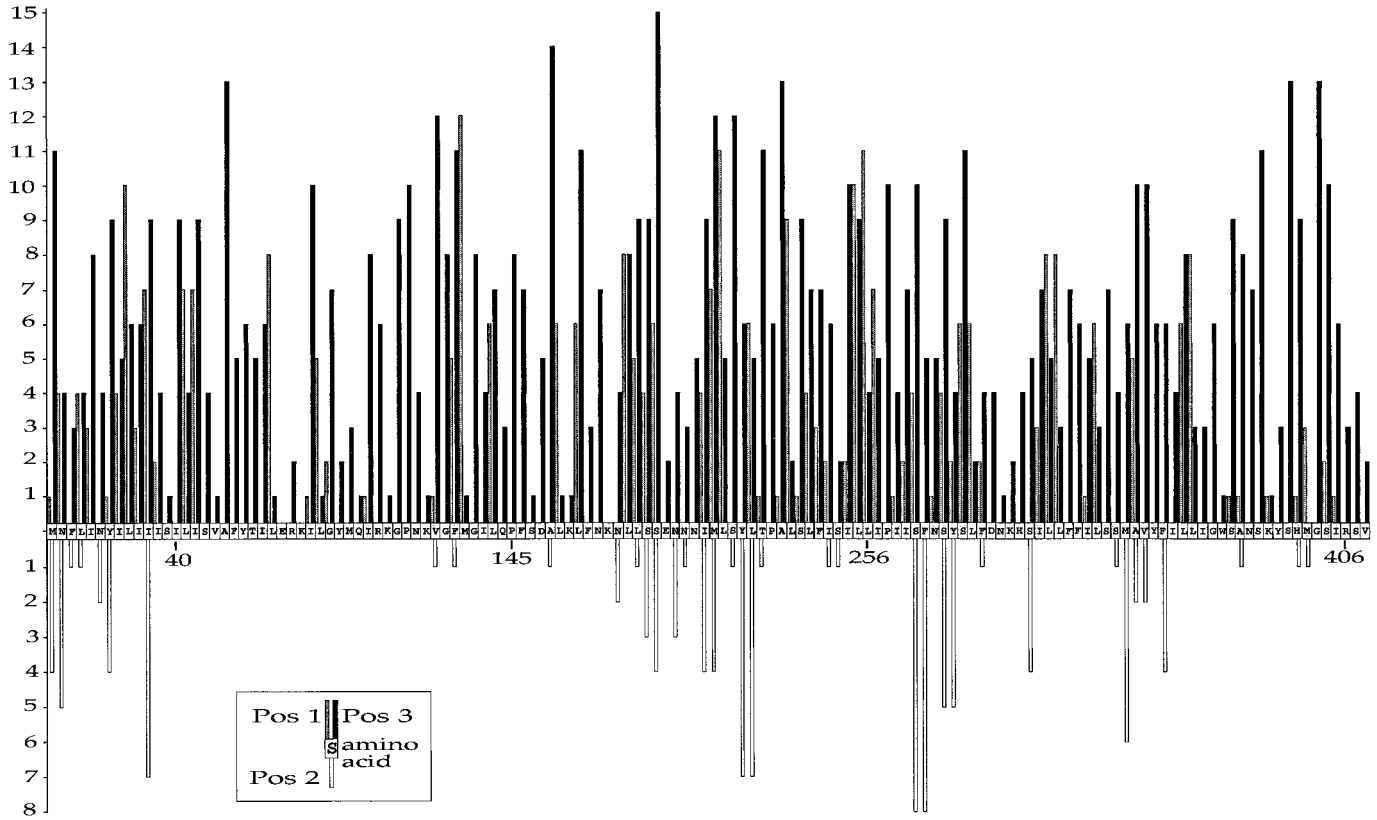

FIG. 6. Nucleotide and amino acid variation for the ND1 gene region. Vertical bars represent minimum number of steps per site, categorized by codon position (1st and 3rd above origin, 2nd below origin). Minimum numbers calculated on most-parsimonious trees for the data using MacClade. Amino acids (in boxes on origin) shown represent a consensus of that observed, with variable residues indicated by shaded boxes. Nucleotides translated assuming the genetic code of *Drosophila* mtDNA, using MacClade.

Phylogenetic Behavior and Utility

Phylogenetic analysis of the dendryphantine CO1 data result in patterns of relationship inconsistent (to different degrees) with those for other data partitions, suggesting conflicting phylogenetic signal. What is the basis of this conflict in signal? As we can be reasonably sure that the CO1 sequences share history with the other linked mitochondrial genes (lacking evidence for nuclearization or sequence contamination), lineage sorting or hybridization scenarios seem unlikely. Also, because the number of CO1 sites is reasonably large, the probability of concentrated conflict resulting from sampling error should be small. More likely, complexities in the evolutionary dynamics of CO1 evolution, beyond those accommodated by the phylogenetic methods used here, are contributing to misleading phylogenetic signal.

We have attempted to account for obvious complexities in standard ways, e.g., via incorporation of within- and among-site rate variation, and some of this accounting appears to have reduced signal conflict. For example, parameter-rich likelihood analyses result in trees with less obvious conflict. Standard parsimony ILD tests are significant; six-parameter parsimony tests are not. In addition to these analyses, we have also assessed the influence of cross-taxa variation in base composition, which is known to potentially mislead phylogeny reconstruction (summarized by Swofford *et al.*, 1996). The impact of this bias was assessed by performing neighbor-joining distance analyses on data transformed to LogDet distances, with and without the incorporation of among-site rate variation (following the various suggestions presented in Swofford *et al.*, 1996). A range of transformations resulted in variation in estimated tree topologies, but all of these trees included clades comprising mixtures of dendryphantine and outgroup taxa (results not shown).

Finally, following the lead of Naylor and Brown (1998), we explored the phylogenetic behavior of different CO1 sites by examining their retention indices (RI) on the three most-parsimonious trees from the unordered combined analysis (Fig. 10). There are no strong indications that sites modally coding for particular amino acids or amino acid classes (e.g., hydrophobic versus hydrophilic, charged versus not) have significantly higher RI's, and hence potentially more phylogenetic information, than others. However, when sites are categorized into classes by codon position and/or

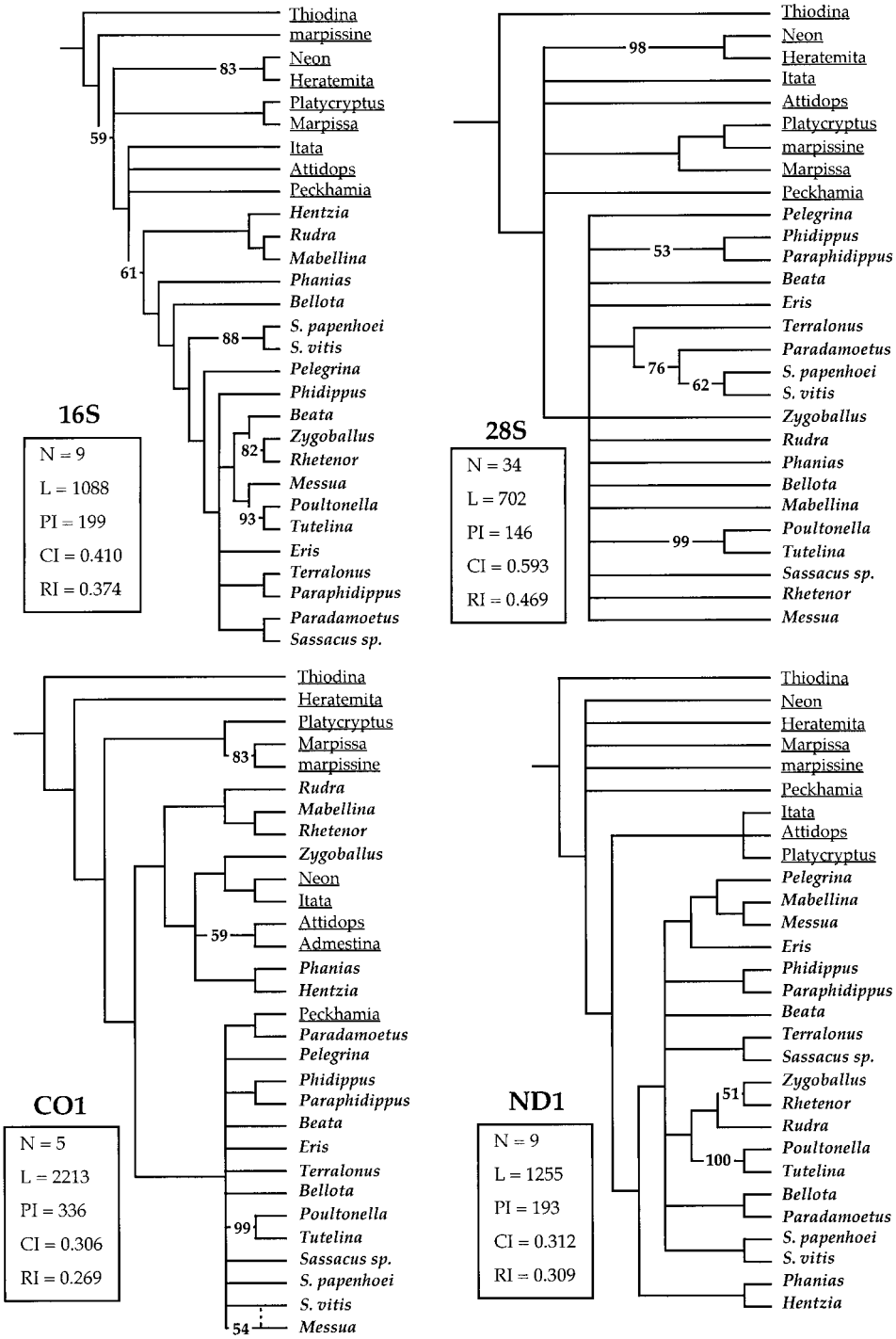

FIG. 7. Strict consensus trees resulting from independent parsimony analyses of four separate data partitions, each analysis comprising a heuristic search with TBR branch-swapping, 1000 random addition search replicates, gaps treated as a fifth state for length-variable partitions. Bootstrap proportion values (on branches) based on 1000 heuristic search replicates, five TBR random addition search sequences per replicate. N, No. of most-parsimonious trees; L, tree length; PI, No. of parsimony-informative characters; CI, consistency index; RI, retention index.

functional domain, there does appear to be a consistent pattern that RI's of parsimony-informative sites from the more conservative classes are lower. That is, in the conservative classes, whereas fewer of the sites may be parsimony informative, those that are show more homoplasy. For instance, protein domains that are most variable (e.g., I2 and I5; Fig. 5) have the highest RI's among parsimony-informative sites (variable, nonau-

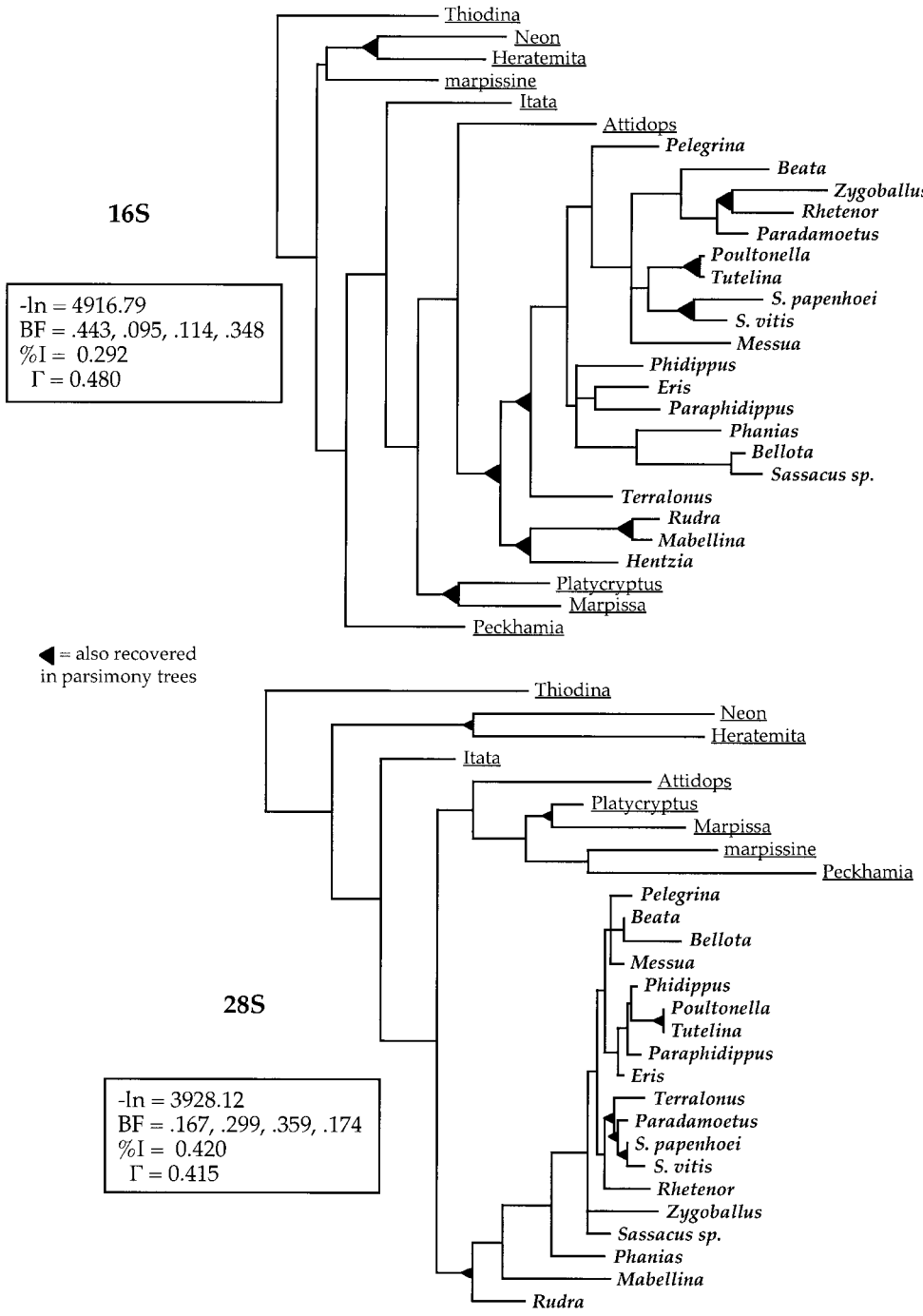

FIG. 8. Maximum-likelihood trees resulting from successive-approximation searches of 16S and 28S data partitions. Searches conducted using best-fit models; initial tree search consisting of a weak heuristic search, parameter estimation and fixation, followed by a thorough heuristic search (see text). Searches were deemed complete when trees of nearly equal likelihood were found in successive iterations. The 16S tree shown is one of three trees of equal likelihood—trees not figured differ in placement of *Messua*, either basal sister to *Beata* clade or basal sister to (*Poultonella*, *S. Papenhoei*) clade. Clades recovered in a majority of parsimony trees highlighted. BF, estimated base frequencies (A, C, G, T); %I, estimated proportion of invariable sites; Γ, estimated gamma shape parameter. Parameter estimates shown are based on the tree figured.

tapomorphic), and the most conservative (e.g., M6 and M8; Fig. 5) have the lowest RI's. Similarly, the more conservative 2nd positions show lower RI's than either 1st or 3rd positions. This would suggest that one shouldn't necessarily expect the most conservative classes of sites to provide the most phylogenetically

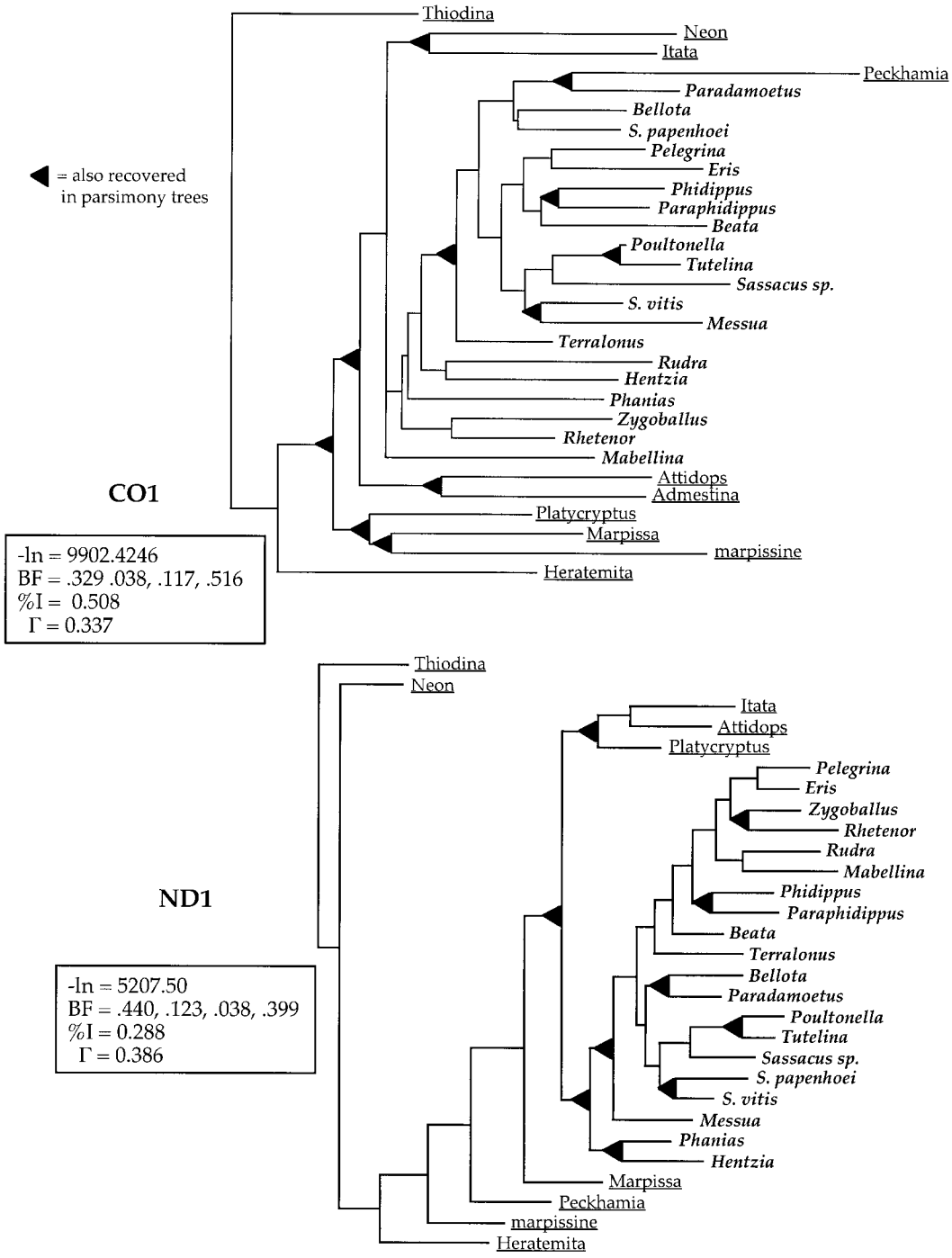

FIG. 9. Maximum-likelihood trees resulting from successive-approximation searches of CO1 and ND1 data partitions. Searches conducted using best-fit models, following iterative approach outlined in text. ND1 tree shown is one of three trees of equal likelihood—trees not figured differ in placement of *Messua*, either basal sister to *Terralonus* clade or basal sister to (*Bellota*, *S. Papenhoei*) clade. CO1 tree shown is one of two trees of equal likelihood, the tree not shown differing in the resolution of the ((*Neon*, *Itata*), *Mabellina*, "all others") trichotomy, with *Mabellina* as the basal member. Clades recovered in a majority of parsimony trees highlighted.

reliable variation (an assumption that we have made in some of our analyses, e.g., no 3rd ILD analyses). More importantly, these results strongly suggest that higher-level interactions (e.g., variable selective constraints at the amino acid level) are influencing the dynamics of CO1 nucleotide evolution and perhaps contributing to conflicting patterns of phylogenetic relationship.

Might we generalize from our dendryphantine data to help inform the design of future spider molecular

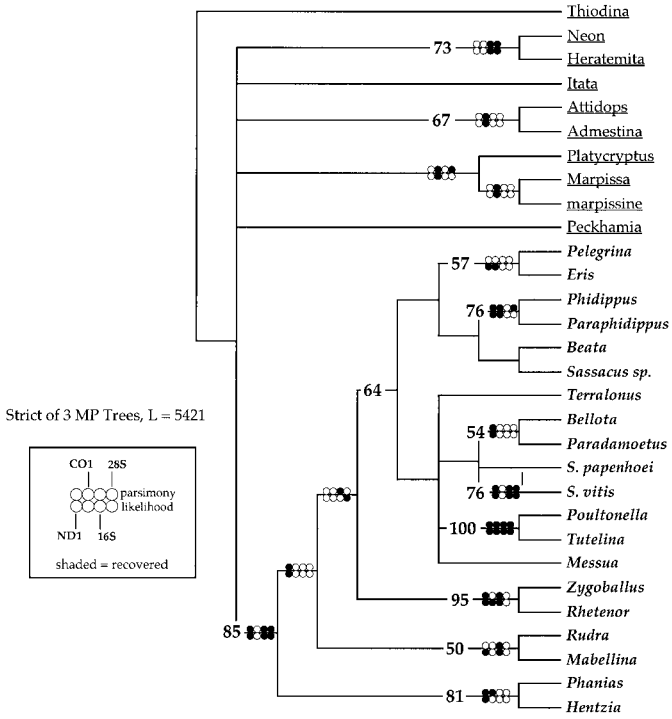

FIG. 10. Strict consensus tree resulting from combined parsimony analysis of all data. Analysis consisted of a heuristic search with TBR branch-swapping, 1000 random addition search replicates, gaps treated as a fifth state for length-variable partitions. Clades recovered in both parsimony and likelihood analyses of individual partitions are indicated on branches, as are BP values (based on 1000 heuristic search replicates, five TBR random addition search sequences per replicate).

phylogenetic projects? We feel that while such extrapolations are potentially helpful, they must also be viewed as preliminary, given that spider molecular phylogenetics is underdeveloped. We tentatively suggest the following. First, it appears that both nuclear and mitochondrial ribosomal sequences are phylogenetically informative at a "generic" level of phylogenetic divergence but are also likely both approaching their limits from opposite directions. Many studies of nonspider taxa show that nuclear 28S sequences are informative at higher levels of divergence (see Hillis and Dixon, 1991), and the dendryphantine data suggest much room for further divergence (i.e., the tree is shallow; see Fig. 8). The limit for these sequences will be at lower levels, although consideration of longer sequences spanning multiple "divergent-domain" regions (see Schnare *et al.*, 1996) might provide some species-level phylogenetic resolution. On the other hand, mitochondrial 16S sequences have been successfully used at the population, species, and generic levels in spiders (Huber *et al.*, 1993; Hedin, 1997b; Bond *et al.*, 2000; Masta, 2000b). Both saturation and alignment difficulties should diminish the utility of this gene region at even higher levels, although conserved regions will retain some utility. It is more difficult to extrapolate from the protein-coding data. Both gene regions are informative at lower levels in spiders (e.g., Hedin, 1997a; Garb, 1999; Gillespie *et al.*, 1997; Masta, 2000b). If we were to consider only overall divergence values (as is often practiced), we might conclude that CO1 would outperform ND1 at generic-level divergences. This does not appear to be the case, and the analyses presented here illustrate how the (perhaps taxon-specific) functional characteristics of protein-coding genes impact phylogenetic utility at higher levels of divergence.

Dendryphantine Evolution

Our molecular data give support to the monophyly of Dendryphantinae, sensu Maddison (1996). We find this result reassuring, especially given that Maddison's exclusion of some genera (*Admestina*, *Attidops*, *Peckhamia*) and inclusion of others (*Mabellina*) had been done with some doubt. In the case of *Mabellina*, its inclusion in Dendryphantinae had not been based on the explicitly proposed synapomorphies, which *Mabel-*

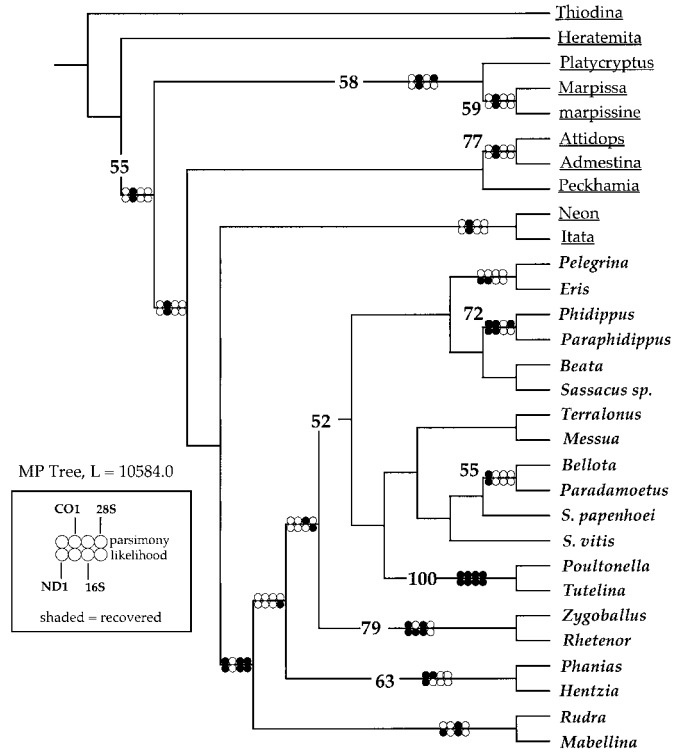

FIG. 11. Most-parsimonious tree resulting from combined parsimony analysis of all data; all partitions except for CO1 treated as "type = unordered," CO1 as "type = LN" (see Table 3). Analysis consisted of a heuristic search with TBR branch-swapping, 1000 random addition search replicates, gaps treated as a fifth state for length-variable partitions. Clades recovered in both parsimony and likelihood analyses of individual partitions are indicated on branches, as are BP values (based on 1000 heuristic search replicates, five TBR random addition search sequences per replicate).

TABLE 3

Results of ILD Tests

	CO1	ND1	16S + tRNA	28S
CO1	—	$P < 0.001$	$P < 0.001$	$P < 0.001$
ND1	**$P = 0.864$** *$P = 0.463$*	—	$P = 0.098$	$P = 0.045$
16S + tRNA	**$P = 0.988$** *$P = 0.494$*	—	—	$P = 0.157$
28S	**$P = 0.953$** *$P = 0.038$*	—	—	—

Note. Results of pairwise ILD tests for each of four data partitions. Each test is based on 1000 data randomizations, each randomization comprising a TBR heuristic search with three random addition sequence replicates. *Admestina* (w/CO1 only) was excluded from all tests, whereas *Hentzia* was excluded from all tests involving 28S data. Invariant characters were removed prior to all tests; tests involving length-variable partitions include gaps treated as a fifth base. Above diagonal: *P* values resulting from tests in which all characters are treated as unordered. Below diagonal: *P* values resulting from tests involving CO1 treated as type = LN, other partitions type = unordered (in boldface), or CO1 1st and 2nd positions only, other partitions type = unordered (in italics). Both sets of searches were constrained to save no more than 500 trees per random addition search replicate. Type = LN corresponds to a symmetric "six-parameter" step matrix. This step matrix was derived by first calculating tree-independent pairwise base differences for all substitution types, using the "Pairwise Base Difference" facility in PAUP*. These values were transformed into weights using the "LN" function presented in Cunningham (1997b), with the cost of going from nucleotide *i* to nucleotide *j* (K_{ij}) equal to $-\ln(X_{ij}/X)$, treating X_{ij} as an average number of changes between *i* and *j* in either direction (from all possible pairwise combinations for 30 taxa) and X as the sum of such averages. These costs are $K_{AG} = 3.1$, $K_{CT} = 4.0$, $K_{AT} = 3.0$, $K_{AC} = 6.2$, $K_{GT} = 4.1$, $K_{CG} = 6.9$.

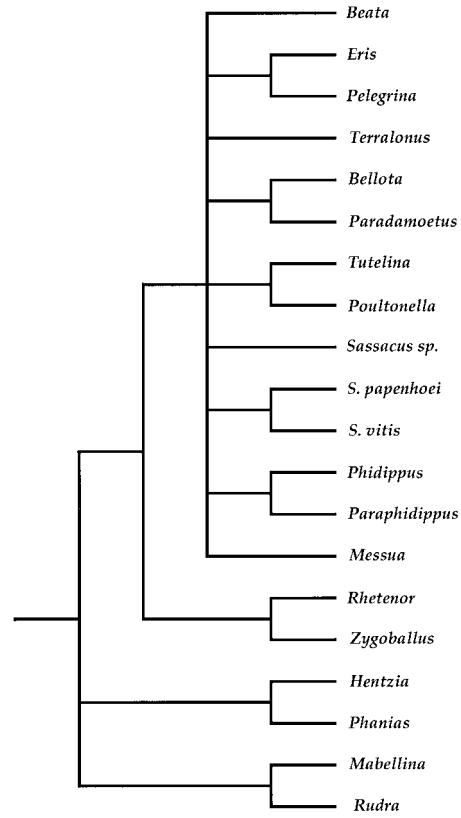

FIG. 12. A conservative summary of Dendryphantine phylogeny based on molecular phylogenetic results.

lina lacks, but rather on a vague sense of overall resemblance in body form and markings (that is, on unarticulated characteristics). The molecular data indicate that the three dendryphantine synapomorphies proposed by Maddison may in fact be valid, and their absence in some dendryphantines can be considered a secondary loss.

Outside the dendryphantines, there is some support for a close relationship between *Neon* and *Heratemita* and between *Attidops* and *Admestina* and some confirmation for the monophyly of the marpissines (Fig. 10). These issues will be dealt with in more detail in our treatment of salticid phylogeny as a whole (M. C. Hedin and W. P. Maddison, unpublished).

A conservative summary of our molecular phylogenetic results within the Dendryphantinae is shown in Fig. 12. Whereas precise details of the deepest structure in the clade have weak support, three separate genes and the combined analyses suggest that at least *Phanias* and *Hentzia,* and possibly also *Rudra* and *Mabellina,* fall outside a clade containing the other dendryphantines sampled (i.e., are "basal"). This accords with Maddison's (1996) suggestion that *Phanias*

TABLE 4

Rate Parameter Estimates

	Transitions		Transversions			
	C<>T	A<>G	A<>T	A<>C	C<>G	G<>T
ND1	19.07	5.08	0.49	0.60	1.48	1
16S + tRNA	93.43	20.37	28.10	11.38	0.00	1
28S	4.18	1.44	1.14	0.80	0.55	1
CO1	66.71	59.94	1.13	0.96	12.71	1

Note. Rate parameters from ML-estimated R-matrices. All estimates based on ML trees (Figs. 8 and 9) using best-fit models.

occupies a basal position among dendryphantines, along with *Hentzia,* because of their retaining the apparently ancestral traits of epiandrous gland fusules and an extra sperm duct loop. *Phanias, Hentzia, Rudra,* and *Mabellina* have more elongate bodies than is typical for dendryphantines and thereby resemble the sister group to the dendryphantines (the marpissines). These four genera also lack the "stereotypical" dendryphantine palpus seen in *Pelegrina, Phidippus, Paraphidippus, Beata, Bellota,* and *Tutelina,* in which the distal part of the embolus is terminally directed and stands abruptly perpendicular against, and narrower than, the laterally directed basal part of the embolus. This suggests that dendryphantines began as rather marpissine-like elongate salticids that only subsequently evolved the "stereotypical" palpus.

The details of relationships within the remaining dendryphantines are largely unclear, except for a few sister relationships. Maddison (1996, p. 225) suggested that *Poultonella* and *Tutelina* are close relatives on the basis of an unusual keel on the inner margin of the chelicera that may be related to ant-feeding (Wing, 1983). Our molecular analyses strongly confirm this relationship. Maddison (1995) suggested that *Rhetenor* may represent an extreme form of *Zygoballus,* and our analyses confirm a close relationship between a Mexican *Rhetenor* and *Zygoballus rufipes* (we note, however, that this conclusion might not apply to the true *Rhetenor,* which is based on a little-known neotropical species). Combined analyses (Figs. 10 and 11) place *Bellota* and *Paradamoetas* as sister groups, suggesting that their antlike appearance may be homologous.

Hill (1979) placed the species previously known as *Metaphidippus vitis* into *Sassacus* on the basis of similarity in scales and courtship behavior with *Sassacus papenhoei.* Maddison (1996) rejected this move as premature because data from only few dendryphantines had been available to Hill, but our molecular data suggest that Hill had in fact been correct (for this reason, we accept his change and refer to the species as *Sassacus vitis*). A close relationship between *S. vitis* and *S. papenhoei* is indicated by three of the four genes. It will be interesting to investigate whether other species, such as *Agassa cyanea* (which, like *S. papenhoei,* resembles a beetle) and *"Pseudicius" siticulosus* (which has courtship behavior like *S. vitis* and *S. papenhoei*) also belong with this group. The neotropical specimen that we identified as *Sassacus* sp. did not fall with the temperate *Sassacus.* Maddison (1996) suggested that the neotropical *Sassacus* belongs elsewhere.

G. B. Edwards (unpublished) proposes dividing the recognized genus *Eris* in two, with *Eris militaris* and a few others remaining in *Eris* and *E. aurantia* transferring back into *Paraphidippus.* On the basis of morphological data, he suggests that *Paraphidippus* may be the sister group to *Phidippus.* Our analyses give independent support to his proposal. We did not sample from the *mannii* group of *Metaphidippus,* which may be near *Eris* (Maddison, 1996).

There are of course many groups of dendryphantines for which we have no species sampled. Among the neotropical genera, we do not have a clear prediction as to where *Lurio, Parnaenus,* and *Gastromicans* might fall, but we expect they will rest within the clade from *Beata* to *Messua* (Fig. 12). This clade may include the bulk of the subfamily, and much denser sampling may be needed before our molecular analyses would resolve its phylogenetic structure. Lacking any sampling of Old World taxa, we can only guess where the three major groups might fall: *Macaroeris* and *Rhene* have the same ancestral features as *Phanias* and thus might also be basal, whereas *Dendryphantes* is likely in the *Beata* to *Messua* clade (Fig. 12).

ACKNOWLEDGMENTS

Generous assistance in sampling specimens was given to us by G. Bodner (*Messua, Admestina, Paraphidippus,* marpissine), G. B. Edwards and R. R. Jackson (*Heratemita*), and E. Hebets (*Hentzia, Poultonella*). Tila María Pérez helped us in obtaining permits and specimens (*Bellota, Mabellina, Paradamoetas, Rhetenor*), which were collected with the assistance of José Luis Castelo, Fernando Alvarez, and G. Bodner. Lab work was carried out in the LMSE, Arizona Research Labs, University of Arizona. R. Bonner, S. Vaught, M. Schwartz, and B. Coullahan of the LMSE DNA sequencing lab were particularly helpful. This work was supported by a fellowship to W.P.M. from the David and Lucile Packard Foundation. Comments of C. Cunningham and two anonymous reviewers greatly improved the manuscript.

REFERENCES

Blest, A. D., and Sigmund, C. (1984). Retinal mosaics of the principal eyes of two primitive jumping spiders, *Yaginumanis* and *Lyssomanes:* Clues to the evolution of Salticid vision. *Proc. R. Soc. Lond. B* **221:** 111–125.

Bond, J. E., Hedin, M. C., Ramirez, M. G., and Opell, B. D. (2001). Deep molecular divergence in the absence of morphological and ecological change in the Californian coastal dune endemic trapdoor spider *Aptostichus simus. Mol. Ecol.,* in press.

Coddington, J. A., and Levi, H. W. (1991). Systematics and evolution of spiders (Araneae). *Annu. Rev. Ecol. Syst.* **22:** 565–592.

Cunningham, C. W. (1997a). Can three incongruence tests predict when data should be combined? *Mol. Biol. Evol.* **14:** 733–740.

Cunningham, C. W. (1997b). Is congruence between data partitions a reliable predictor of phylogenetic accuracy? Empirically testing an iterative procedure for choosing among phylogenetic methods. *Syst. Biol.* **46:** 464–478.

Cunningham, C. W., Zhu, H., and Hillis, D. M. (1998). Best-fit maximum-likelihood models for phylogenetic inference: Empirical tests with known phylogenies. *Evolution* **52:** 978–987.

Farris, J. S., Kallersjo, M., Kluge, A. G., and Bult, C. (1995). Testing significance of incongruence. *Cladistics* **10:** 315–319.

Felsenstein, J. (1985). Confidence limits on phylogenies: An approach using the bootstrap. *Evolution* **39:** 783–791.

Garb, J. E. (1999). An adaptive radiation of Hawaiian Thomisidae: Biogeographic and genetic evidence. *J. Arachnol.* **27:** 71–78.

Gilbert, D. (1992). SeqApp, version 1.9a. Indiana Univ., Bloomington.

Gillespie, R. G., Croom, H. B., and Hasty, G. L. (1997). Phylogenetic relationships and adaptive shifts among major clades of *Tetragnatha* spiders (Araneae: Tetragnathidae) in Hawai'i. *Pacific Sci.* **51:** 380–394.

Hedin, M. C. (1997a). Molecular phylogenetics at the population/species interface in cave spiders of the southern Appalachians (Araneae: Nesticidae: *Nesticus*). *Mol. Biol. Evol.* **14:** 309–324.

Hedin, M. C. (1997b). Speciational history in a diverse clade of habitat-specialized spiders (Araneae: Nesticidae: *Nesticus*): Inferences from geographic-based sampling. *Evolution* **51:** 1927–1943.

Higgins, D. G., and Sharp, P. M. (1988). Clustal: A package for performing multiple sequence alignment on a microcomputer. *Gene* **73:** 237–244.

Hill, D. E. (1979). The scales of salticid spiders. *Zool. J. Linn. Soc.* **65:** 193–218.

Hillis, D. M., and Dixon, M. T. (1991). Ribosomal DNA: Molecular evolution and phylogenetic inference. *Q. Rev. Biol.* **66:** 411–453.

Huber, K. C., Haider, T. S., Muller, M. W., Huber, B. A., Schweyen, R. J., and Barth, F. G. (1993). DNA sequence data indicates the polyphyly of the family Ctenidae (Araneae). *J. Arachnol.* **21:** 194–201.

Jackson, R. R. (1982). The behavior of communicating in jumping spiders (Salticidae). *In* "Spider Communication: Mechanisms and Ecological Significance" (P. N. Witt and J. S. Rovner, Eds.), pp. 213–247. Princeton Univ. Press, Princeton, NJ.

Jackson, R. R. (1986). Web building, predatory versatility, and the evolution of the Salticidae. *In* "Spiders: Webs, Behavior, and Evolution" (W. A. Shear, Ed.), pp. 232–268. Stanford Univ. Press, Stanford, CA.

Jackson, R. R., and Pollard, S. D. (1996). Predatory behavior of jumping spiders. *Annu. Rev. Entomol.* **41:** 287–308.

Lunt, D. H., Zhang, D.-X., Szymura, J. M., and Hewitt, G. M. (1996). The insect cytochrome oxidase I gene: Evolutionary patterns and conserved primers for phylogenetic studies. *Insect Mol. Biol.* **5:** 153–165.

Maddison, D. R., and Maddison, W. P. (1999). MacClade 4, test version 4.0 beta. Version 4.0 to be published by Sinauer, Sunderland, MA.

Maddison, W. P. (1987). *Marchena* and other jumping spiders with an apparent leg-carapace stridulatory mechanism (Araneae: Salticidae: Heliophaninae and Thiodininae). *Bull. Br. Arachnol. Soc.* **7:** 101–106.

Maddison, W. P. (1988). "A Revision of Jumping Spider Species Groups Formerly Placed in the Genus *Metaphidippus*, with a Discussion of Salticid Phylogeny (Araneae)." Ph.D. thesis, Harvard University, Cambridge, MA.

Maddison, W. P. (1995). *Rhetenor*, one of the Salticidae pages in the "Tree of Life Project" (D. Maddison, Ed.). http://spiders.arizona.edu/salticidae/rhetenor/rhetenor.html

Maddison, W. P. (1996). *Pelegrina* Franganillo and other jumping spiders formerly placed in the genus *Metaphidippus* (Araneae: Salticidae). *Bull. Mus. Comp. Zool.* **154:** 215–368.

Masta, S. (2000a). Mitochondrial sequence evolution in spiders: Intraspecific variation in tRNAs lacking the TΨC arm. *Mol. Biol. Evol.* **17:** 1091–1100.

Masta, S. (2000b). Phylogeography of the jumping spider *Habronattus pugillis* (Araneae: Salticidae): Recent vicariance of sky island populations? *Evolution.* **54:** 1699–1711.

Naylor, G. J. P., and Brown, W. M. (1998). *Amphioxus* mitochondrial DNA, chordate phylogeny, and the limits of inference based on comparisons of sequences. *Syst. Biol.* **47:** 61–76.

Poe, S. (1996). Data set incongruence and the phylogeny of Crocodilians. *Syst. Biol.* **45:** 393–414.

Posada, D., and Crandall, K. A. (1998). MODELTEST: Testing the model of DNA substitution. *Bioinformatics* **14:** 817–818.

Proszynski, J. (1976). Studium systematyczno-zoogeograficzne and rodzina Salticidae (Aranei) Regionow Palearktycznego i Nearktycznego. *Wyzsza Szkola Pedagogiczna Siedlcach Rozprawy* **6:** 1–260.

Sambrook, J., Fritsch, E. F., and Maniatis, T. (1989). "Molecular Cloning: A Laboratory Manual," Cold Spring Harbor Laboratory Press, Cold Spring Harbor, NY.

Schnare, M. N., Damberger, S. H., Gray, M. W., and Gutell, R. R. (1996). Comprehensive comparison of structural characteristics in eukaryotic cytoplasmic large subunit (23S-like) ribosomal RNA. *J. Mol. Biol.* **256:** 701–719.

Shahjahan, R. M., Hughes, K. J., Leopold, R. A., and DeVault, J. D. (1995). Lower incubation temperature increases yield of insect genomic DNA isolated by the CTAB method. *Biotechniques* **19:** 333–334.

Simon, C., Frati, F., Beckenbach, A., Crespi, B., Liu, H., and Flook, P. (1994). Evolution, weighting, and phylogenetic utility of mitochondrial gene sequences and a compilation of conserved polymerase chain reaction primers. *Ann. Entomol. Soc. Am.* **87:** 651–701.

Simon, E. (1901). "Histoire Naturelle des Araignées," 2nd ed., Vol. 2, Paris.

Simon, E. (1903). "Histoire Naturelle des Araignées," 2nd ed., Vol. 2, Paris.

Swofford, D. L. (1999). PAUP*. Phylogenetic Analysis Using Parsimony (*and Other Methods). Version 4. Sinauer, Sunderland, MA.

Swofford, D. L., Olsen, G. J., Waddell, P. J., and Hillis, D. M. (1996). Phylogenetic inference. *In* "Molecular Systematics" (D. M. Hillis, C. Moritz, and B. K. Mable, Eds.), 2nd ed., pp. 407–514. Sinauer, Sunderland, MA.

Thornton, J. W., and DeSalle, R. (2000). A new method to localize and test the significance of incongruence: Detecting domain shuffling in the nuclear receptor superfamily. *Syst. Biol.* **49:** 183–201.

Wanless, F. R. (1984). A review of the spider subfamily Spartaeinae nom. n. (Araneae: Salticidae) with descriptions of six new genera. *Bull. Br. Mus. Nat. Hist. Zool.* **46:** 135–205.

Wheeler, W. C., Gatesy, J., and DeSalle, R. (1995). Elision: A method for accommodating multiple molecular sequence alignments with alignment-ambiguous sites. *Mol. Phylogenet. Evol.* **4:** 1–9.

Wing, K. (1983). *Tutelina similis* (Araneae, Salticidae)—An ant mimic that feeds on ants. *J. Kansas Entomol. Soc.* **56:** 55–58.

Yang, Z. (1994). Maximum likelihood phylogenetic estimation from DNA sequences with variable rates over sites: Approximate methods. *J. Mol. Evol.* **39:** 306–314.